JAAS



PAPER

View Article Online
View Journal | View Issue



Cite this: *J. Anal. At. Spectrom.*, 2023, **38**, 2656

Non-target analysis and characterisation of nanoparticles in spirits *via* single particle ICP-TOF-MS†

Raquel Gonzalez de Vega, [©] ^a Thomas E. Lockwood, [©] ^b Lhiam Paton, ^a Lukas Schlatt^c and David Clases [©] *^a

Nanoparticles (NPs) can be found throughout our direct environment as well as in a large range of consumer products. However, there is a lack of data on abundances and properties, which requires dedicated methods to identify and characterise NP entities. Single particle inductively coupled plasmamass spectrometry (SP ICP-MS) is becoming one of the most relevant methods for counting NPs and studying NP composition and properties. Especially time-of-flight (TOF) technology for ICP-MS holds the key to study single particle composition and to perform non-target particle screening. This is achieved through the unique detection paradigm in TOF acquiring all isotopes across the periodic table at 35 kHz and faster. Nevertheless, non-targeted screening methods face limitations due to two factors. First, large data sets challenge data processing units and require substantial time, and second, for each isotope/element, a decision limit to distinguish between random noise and a SP signal has to be established. Here, we propose a novel lognormal approximation method to rapidly model background levels and decision limits. This method was integrated in a pre-analysis tool which detected SP data signatures of all m/z recorded via SP ICP-TOF-MS. Within seconds, particulate elements could be pinpointed in large data files and selected for more dedicated characterisation steps. In a proof of concept, we used this non-target screening method to identify inorganic NPs in selected samples of whisky, vodka, gin, and liqueur. Following qualitative analyses, number concentrations, compositions, masses, and size distributions were investigated. Besides Mn, Fe and Cu as expected NP entities, Ti, Aq, Au and Sn-based particles were found in investigated samples.

Received 29th July 2023 Accepted 25th October 2023

DOI: 10.1039/d3ja00253e

rsc.li/jaas

Introduction

Nanoparticles (NPs) have been present ubiquitously since the beginning of the Earth and have played an important role during its development. They have a vast impact on our lives and immediate surroundings, but we are struggeling to decipher all their properties and traits. Despite their first scientific consideration going back to the 1850s, they received only little attention for the years to come which was at least partially attributed to a lack of analytical capability. However nowadays, they are driving innovation in various scientific disciplines and are increasingly integrated in new materials. While this is certainly inspired by our improving capability to characterise

The development of single particle inductively coupled plasmamass spectrometry (SP ICP-MS) was a turning point for NP analyses. It combines high counting rates with elemental analysis and can produce models on PNCs as well as on particle masses and sizes when suitable standards are analysed concurrently. The concept of SP ICP-MS is based on the analysis of NPs at low number concentrations to ensure the introduction of individual particles into the plasma. Here, single particles are atomised and elemental cations are formed. These are subsequentially extracted in discrete ion clouds for mass spectrometry and detected as time

NPs, suitable analytical methods are still a bottleneck for expanding our knowledge on emerging nanomaterials. Techniques are required to detect individual NPs at high counting rates and further characterise them regarding size, mass, composition, structure, and stability. Several methods have been developed to enable the characterisation of NPs such as nanoparticle tracking analysis (NTA), dynamic light scattering (DLS), and electron microscopy (EM).^{4,5} While these techniques are well suited to describe certain facets of NPs, they are not capable of establishing comprehensive and accurate models on particle number concentrations (PNC), size/mass distributions and/or compositions.

[&]quot;Institute of Chemistry, University of Graz, Graz, Austria. E-mail: David.Clases@uni-graz.at

 $[^]b$ Hyphenated Mass Spectrometry Laboratory, University of Technology Sydney, NSW, Australia

^cNu Instruments, Wrexham, UK

[†] Electronic supplementary information (ESI) available: A figure on the single particle Fe isotope ratios, a table comprising all determined SP-data, and the used python script for non-target screening. See DOI: https://doi.org/10.1039/d3ja00253e

Open Access Article. Published on 31 2023. Downloaded on 2025/10/26 11:24:46.

This article is licensed under a Creative Commons Attribution 3.0 Unported Licence.

Paper

resolved pulses. Rapid mass analysers and detectors enable the counting of several hundreds of NPs per minute whilst recording extracted ion clouds from SP events with several data points at integrations times of 100 μs or below. 6,7

The maturation of time-of-flight (TOF) technology for ICP-MS initiated a paradigm shift for the characterisation of individual particles. Previous mass analysers such as quadrupoles scanned sequentially and were limited by their speed, which restricted acquisitions to solely one selected isotope or small mass windows.8,9 As such, non-target approaches were depending on procedures to detect a statistically significant number of NP signals for one element for a set period before analysing the next. Consequently, screening procedures were time and sample consuming, and methodologies could still only target one isotope per detected particle.8 However, SP ICP-TOF-MS enables the rapid and continuous recording of full mass spectra at acquisition rates exceeding 10 kHz. While collision/reaction cells (CRCs) are typically employed to remove confounding ion species, the increased mass resolution of TOF analysers can help additionally to resolve interferences from analyte signals.10

Although SP ICP-TOF-MS may not reach the size detection limits (sDL) of quadrupole and sector-field-based methods, its multi-elemental capabilities permit non-target approaches and investigations on the composition of individual particles. However, the resulting data sets are considerably large and screening efforts are hampered by the ability to carry out data processing sufficiently fast. In this work, we present a rapid nontarget screening method for inorganic NPs via SP ICP-TOF-MS. We developed an algorithm for the pre-analysis of data sets before applying dedicated algorithms for signal accumulation, and calibration processes. In this proof of concept, we selected spirits as complex samples that are exposed to varying conditions and materials during fermentation, distillation and storage. We anticipated that these steps were inherent with the formation or leaching of NP entities. Whisky, gin, vodka, and liqueur samples were selected as a few of the most popular spirit-based drinks and were subjected to the screening method. Identified NP entities were subsequently analysed regarding PNCs, composition and their distributions in mass and size. While this approach may be relevant for toxicological considerations, multielement analysis of ionic and particulate elements may be useful to confirm authenticity as well as to trace adulterations. The production of spirits is often connected to considerable effort and cost from the dedicated ingredients, manufacturing steps and extended maturation or storage procedures. While key components in different spirits have been investigated in profiling efforts to confirm authenticity and to recognise adulterations, 11-18 no data is available regarding particulate analytes.

Materials and methods

Consumables and sample preparation

Element standards (1000 μg mL⁻¹, Single-Element ICP-Standard-Solution Roti®Star) were diluted to working concentrations using ultra-pure water (18.2 M Ω cm, Merck Millipore, Bedford, USA). Calibrations with ionic solutions were

Table 1 Overview and specifics of spirit samples

Sample	Details
W1	Mackmyra Bjorks, Swedish single malt whisky
W2	Talisker, single malt Scotch whisky, aged 10 years
W3	Longrow, peated single malt Scotch whisky
W4	Mackmyra Destination, Swedish single malt whisky
W5	Suntory Whisky Toki, blended Japanese whisky
W6	Speyside single malt Scotch whisky, aged 14 years
W7	Dewar's, blended Scotch whisky, aged 15 years
V1	Zubrowka, Bison Grass Vodka, Poland
G1	Bombay Sapphire, dry gin, England
L1	Amaretto, Il Barone, Italy
L2	Kruska, Kravica, Croatia

performed by using a Merck IV standard (Rahway, New Jersey, US) that was spiked with additional elements (Ti, Au and Sn) found during the screening processes. The calibration mix was diluted to concentrations between 1 ng g $^{-1}$ and 20 ng g $^{-1}$. A 79 \pm 9 nm Au–Ag core–shell (14 nm Ag–51 nm Au–14 Ag nm) was bought in 2 mM citrate from nanoComposix and characterised regarding size distribution, mass concentration, optical properties, surface potential and hydrodynamic radius by the manufacturer.

Analysed spirits are listed in Table 1 and were obtained from local distributors. They were diluted 1:10 in ultra-pure water to limit matrix effects and enable direct analysis. The effects of the low remaining ethanol content was tested by comparing sensitivity of screened elements in ultrapure water and in 4% ethanol, respectively. Values deviated for the targeted elements only slightly (in average 2.7%) rendering more dedicated matrix-matching unnecessary.

Instrumentation and data processing

A Vitesse ICP-TOF-MS platform by Nu Instruments (Wrexham, UK) was operated in single particle mode and recorded and binned mass spectra from 45–210 amu every 96 μs (4 spectra binning) before saving data to disc. Each sample, blank and calibration standard were recorded for 100 s. Cones for liquid sample introduction were installed and the sample uptake rate was set to 0.4 mL min⁻¹. The plasma was operated at 1.35 kW, helium (12 mL min⁻¹) and hydrogen (6 mL min⁻¹) were used as cell gases. The nebuliser flow rate was tuned to provide highest sensitivities while maintaining a CeO/Ce ratio below 5%. The aerosol's transport efficiency using a concentric nebuliser and a cyclonic spray chamber was determined to be 1.76% analysing the core–shell NP standard while considering its known Au mass

Results and discussion

Considerations for non-target approaches via SP ICP-TOF-MS

SP ICP-TOF-MS enables the rapid acquisition of full mass spectra, which is a prerequisite for fast non-target screenings for particulate elements. This potential is somewhat hampered by data files with sizes of several gigabytes per sample. Dedicated processing algorithms often employ various and iterative

JAAS Paper

data processing steps to find SP signals, fit and smooth raw data, accumulate data points of individual SP signals, perform calibrations (mass, size, compositions), calculate relevant parameters (limits of detection (LOD), determine transport efficiency, ionic response, etc.) and visualise data (histograms, principle component analysis, charts, etc.). 19 These procedures are repeated for all acquired elements in all analysed samples. Therefore, data analysis is associated with considerable processing power and time. However, the decision on whether a NP signal has been detected follows relatively simple paradigms and advanced data treatment is not required to indicate elements with SP data signatures.

To decide whether a particle has been detected or not requires statistical measures and is subject to two types of errors: false positive decisions (type I error, rate α) and false negative decision (type II error, rate β). Here, α and β are used to represent the probabilities of data being misinterpreted as a NP or a NP detection being missed. These errors enable to set underlying analytical limits: a decision limit based on an a posteriori assessment whether a NP has been detected, a detection limit to indicate the reliability of an a priori threshold as well as the quantification limit to provide a quantitative estimate.20 At low background levels, the decision limit is solely defined over the α -error and the mean of data set and can be used to count NP detection events over the critical value with a certainty of $1 - \alpha$. This approach requires a minimum of processing power and can be applied to TOF data sets efficiently.

The rapid mass spectra acquisition of m/z in SP ICP-TOF-MS requires the application of a sub-nanosecond analogue-todigital conversion ion detector which somewhat complicates the modelling of background and decision limit. For large background values, a Gaussian-like distribution can be assumed and therefore, Gaussian statistics are used for thresholding. However, low background values do not follow a normal distribution. Unlike for quadrupole-based SP ICP-MS with secondary electron multiplier detectors, data produced by a SP ICP-TOF-MS is also not Poisson distributed and background thresholding cannot rely on Poisson statistics.21 Different elemental ions have varying sensitivities and produce a signal distribution which is subsequently calibrated into "counts". This leads to non-integer intensity values and further, the rapid sub-nanosecond acquisition involves accumulation of multiple spectra before writing data to the disk. For low backgrounds, this can be modelled using a compound Poisson distribution that considers the single ion signal area (SIA). 22-24

To enable non-target NP analysis, we propose an algorithm, which first decides whether to use Gaussian or compound Poisson statistics. The former was used when all data points were above 5 cts and the decision limit was selected as $\mu + 5\sigma$. When mean background levels were low, compound Poisson statistics were approximated using a lognormal (LN) approximation methods as follows: a Poisson distribution with an expected rate (λ) equal to the signal mean was created. Only Poisson events k in the Poisson distribution with k > 0 and P(k) > 00.0001% were considered and approximated with the LN approach. For each value of k a LN distribution with a mean of k was then approximated from the sum of k LN distributions, each with a mean of 1 and a shape parameter determined from a LN fit of the SIA.25 This approximates the distribution produced by sampling the SIA k times, as happens in multi-ion events. The cumulative density function of each LN was then weighted by the Poisson probability of k and summed. The decision limit was then determined as the first value at which the summed cumulative distribution was greater than the desired zero-truncated quantile. This LN approximation method matched results produced by Poisson sampling the SIA as shown in Fig. 1, being significantly faster and only requiring knowledge of the shape parameter of a LN fit of the SIA (in this case 0.47). Given that files can reach the size of several gigabytes, screenings were further accelerated by limiting the number of evaluated data to the first 500 000 data points for each element. Elements within the mass window of 45-210 amu with at least 25 ppm of data points above the respective decision limits were reported and were then selected for in-depth characterisation. The interested reader will find the underlying python script for this non-target approach in the ESI† and online.

Non target analysis of nanoparticles and qualitative evaluation

Table 2 shows an overview of analysed samples and the NPs identified using the screening approach. Each data file had a size of 2 GB, and the developed screening enabled an identification of relevant NP entities with data points above the 25 ppm threshold within seconds. Seven different whisky samples (W1-7), one vodka (V1), one gin (G1) and two liqueur samples (L1-2) were analysed. Ultra-pure water was analysed as blank and contained only negligible amounts of NPs. Tap water was analysed to determine which NPs would typically occur in drinking-grade water. The non-target screening approach in spirits returned a range of NP signals for the elements Sn, Fe, Ti, Ag, Au, Cu, Zn and Mn.

Quantitative characterisation of spirit samples

Elements identified via the non-target screening were analysed quantitatively and the number of detected NPs was calibrated to PNCs as outlined previously.19 Fig. 2 lists the total number of particles detected in each sample and shows pie charts which depict the relative contribution (in %) of the respective particulate elements to that number concentration. All detected NP signals were analysed for coinciding element signals, but no correlations were found. Therefore, the following considerations assumed that detected NP consisted only of one metal, with no other metals present with masses above the detection limit. For Ti, Sn, Cu, Fe and Zn, common oxide phases (TiO₂, SnO_2 , CuO, Fe_2O_3 , and ZnO) were assumed to calculate NP mass and size distributions. PNCs ranged between 9.9×10^3 and 1.23 \times 10⁵ NP per mL. Fe containing NPs were detected in all samples in fractions between 11.5 and 81.4%. All whisky (W1-W7) samples contained Ag and Au NPs at fractions between 6.7 and 31.8% and 5.8 and 30.0%, respectively. Ti-containing NPs were found in the seven whisky samples and the two liquors

Paper JAAS

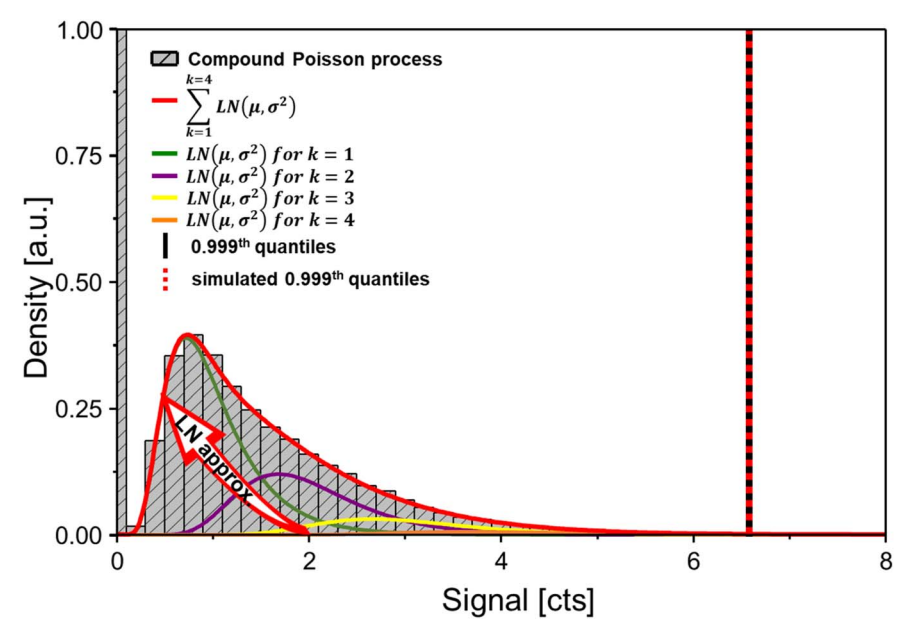


Fig. 1 Comparison of the log-normal approximation and data produced from Poisson sampling of the single-ion distribution. The LN distributions for each Poisson event above zero are shown in red, with the sum approximating the non-zero signal. The 0.999th quantile for the data set and LN approximation are shown as vertical black and red (dotted) lines.

Table 2 Elements identified in single particles

Sample	Elements found at a NP detection score ≥25 ppm
Tap water	Fe, Cu, Zn
W1	Ti, Fe, Ag, Au
W2	Ti, Fe, Ag, Sn, Au
W3	Ti, Mn, Fe, Ag, Sn, Au
W4	Ti, Mn, Fe, Ag, Au
W5	Ti, Mn, Fe, Ag, Au
W6	Ti, Fe, Ag, Au
W7	Ti, Fe, Ag, Au
V1	Fe, Sn
G1	Fe, Cu, Sn
L1	Ti, Mn, Fe, Ag, Sn, Au
L2	Ti, Mn, Fe, Ag

analysed with relative fractions between 4.8 and 36.1%. Sn- and Mn-containing NPs were detected in 5 spirits with relative fractions between 4.7 and 55.8% and 1.2 and 18.2%, respectively. The gin sample was the only spirit containing detectable Cu particles (39.4%).

The signals of detected particulate elements were subsequently evaluated for potential interferences. However, the application of a CRC and He/H₂ cell gas flows enabled the attenuation of most polyatomic interferences and significant levels of naturally abundant isobars were ruled out following the interrogation of isotopic abundances, as demonstrated for Ti in Fig. 3. Fig. 3A shows the transient analysis of 4 selected isotopes ⁴⁸Ti, ¹⁰⁷Ag, ¹²⁰Sn and ¹⁹⁷Au in W3 as a representative sample. ⁴⁸Ti (isotopic abundance: 73.7%) is often interfered by the isobaric ⁴⁸Ca interference and sequentially operating mass

analysers are usually set to target the less abundant ⁴⁷Ti (7.4%) to avoid confounding Ca isotopes and to ensure accurate analysis, although sensitivity decreases drastically. The use of a TOF mass analyser enabled the simultaneous analysis of all isotopes across the selected mass range and allowed the interrogation of isotope ratios to indicate the presence of spectral interferences. Fig. 3B shows the analysis of all Ti isotopes in a single NP signal event and was used to determine relative isotopic abundances. Fig. 3C shows the resulting 47Ti/48Ti ratios for all detected Ti NPs and data was fitted with a linear function to return a slope of 0.105 as experimental isotope ratio, which was in line with the natural ratio of 0.103. As such, no ⁴⁸Ca interference was evident and 48Ti was targeted to benefit from the higher sensitivity. This approach was applied for all analysed polyisotopic elements and isotope ratios were consistent with theoretical values except for Fe, for which the experimental abundance of ⁵⁶Fe was significantly biased. Large particles especially deviated regarding isotope ratios, which was a result from a limited dynamic range. However, other Fe isotopic abundance were in line with theoretical values as shown in Fig. S1 in the ESI.† Therefore, the ⁵⁶Fe isotope was solely considered to determine PNCs and 54Fe was used to determine size and mass distributions.

The non-target screening found Sn NPs in multiple samples and calculations considered Sn $^{4+}$ as most common oxidation state in an oxide phase with a mass fraction of 0.788. Considering each particulate event allowed to model size and mass distributions in histograms. An example is shown for sample W2, which contained the highest number concentrations of SnO₂ NPs (39 500 \pm 1800 mL $^{-1}$). The SnO₂ mass and size distributions in this sample are shown in Fig. 4 and data on other elements is available in Table S1.† For this sample, the mean SnO₂ NP mass was 3.5 ± 4.2 fg, the

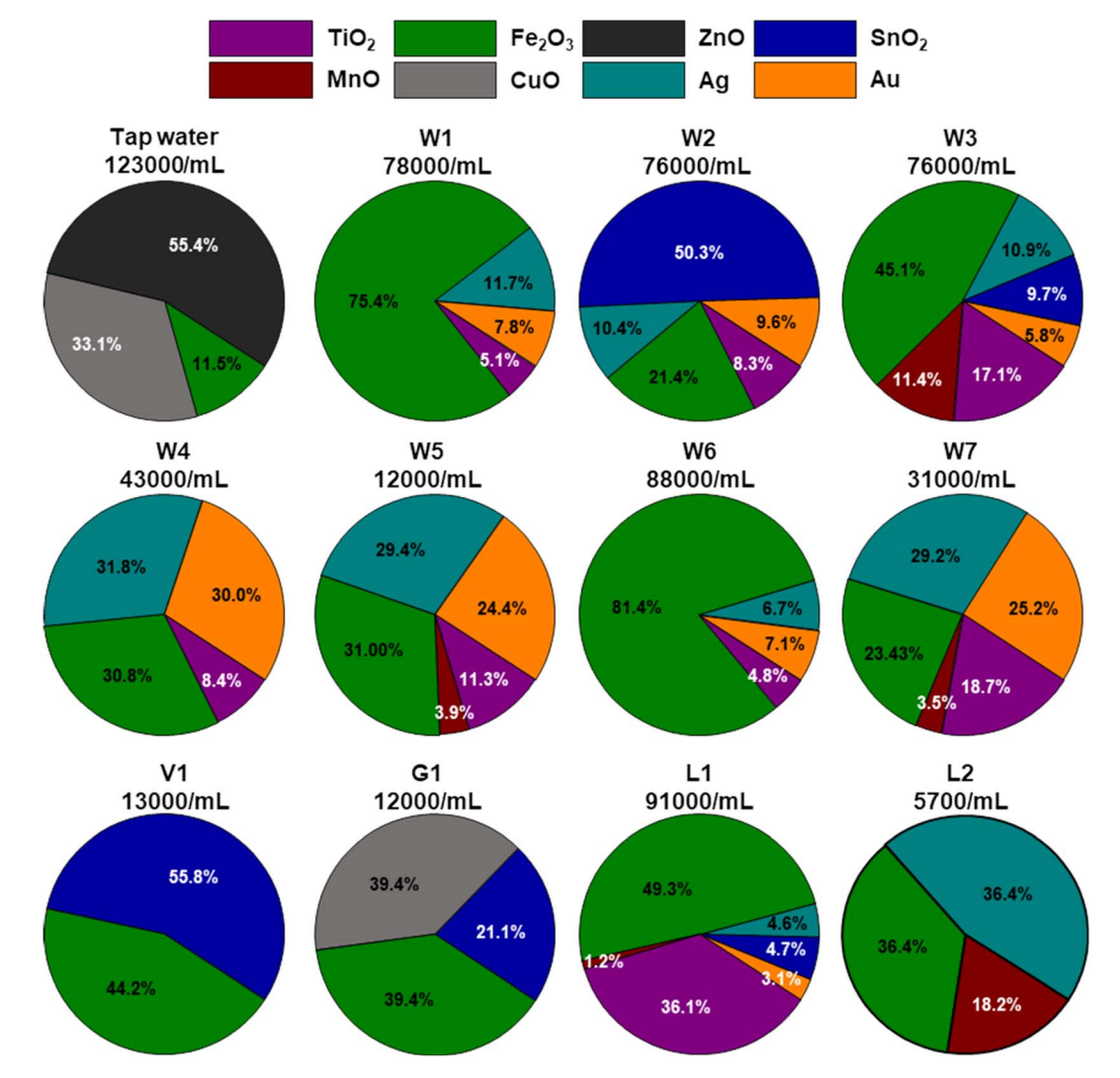


Fig. 2 Overview of PNCs and relative contributions of the different NP entities expressed in %.

mean size was calculated to be 89 \pm 29 nm and the size detection limit was 39 nm.

Across all samples, ionic background levels for Cu, Fe and Mn were relatively high and were assumed to arise from contact with distillation and container materials or from drinking water sources. Detectable Fe₂O₃ sizes were relatively variable and were smallest in tap water (58.6 \pm 24.3 nm) ranging up to 300 \pm 112 nm for sample W3. Mean TiO₂ sizes varied between 80.4 \pm 45.5 nm (W4) and 148 \pm 54 nm (L1). Ag NPs were detectable in samples where Au NP were detectable as well. Only sample L2 contained Ag NPs but no Au NPs. Au and Ag NPs and exhibited relatively consistent sizes between 30.7 and 44.4 nm and, 27.4 and 36.0 nm, respectively. Mean SnO₂ NPs sizes were between 133 and 169 nm. The mean sizes and standard deviations of Au, Ag, MnO, SnO₂, Fe₂O₃ and TiO₂ across all samples are illustrated in Fig. 5. More details on absolute PNCs, ionic background, mean masses, sizes, standard deviations, and figures of merit are listed in Table S1.†

It is unlikely that detected NPs have toxicological implications as absolute PNCs are in a comparably low range when for example compared against drinking (tap) water. Particles based on elements such as Sn, Ag, Fe and Cu have previously been described in tap water and have likely a natural or incidental origin (e.g., plumbing or previous treatment processes).26 It is possible that particles found in spirits originate from different drinking water sources, are a result from leaching processes (e.g., from the distillation process, or during storage), or are intentionally included as additive to improve organoleptic properties.27 Knowledge on the levels and properties of ionic and particulate elements may be useful to confirm authenticity of expensive and elaborated spirits. While element profiles have been investigated for this purpose in the past, 16,17 distinguishing between particulate and ionic entities as well as comparing numbers, compositions and sizes may add additional dimensions which facilitate discrimination between different spirits as well as to carry out provenance analysis. However, this needs to be evaluated by targeting a larger sample size consisting of different brands from various areas and countries.

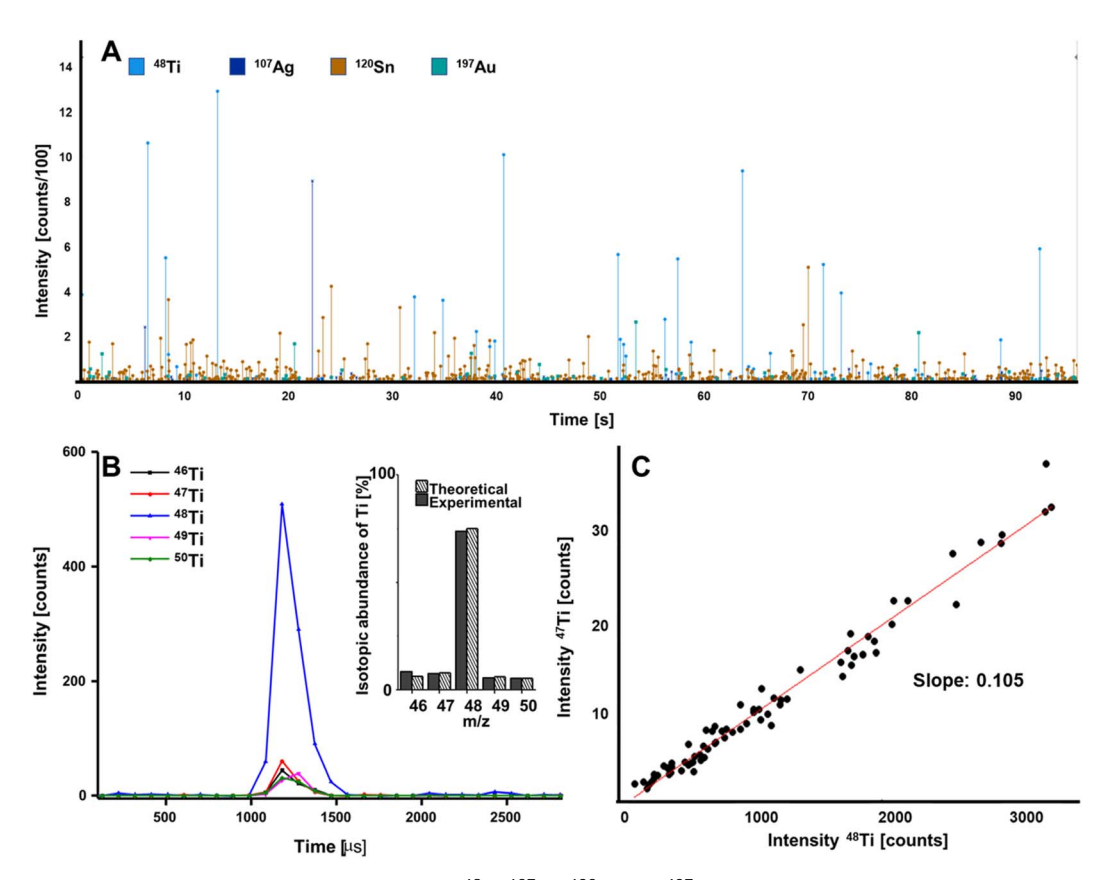


Fig. 3 (A) Transient raw data obtained in SP ICP-TOF-MS for 48 Ti, 107 Ag, 120 Sn and 197 Au in sample W3. (B) The multi-isotopic capabilities of SP ICP-TOF-MS enabled the determination of isotope ratios in individual particles and their comparison against theoretical values. (C) The 47 Ti/ 48 Ti isotope ratios of all detected Ti particles is compared. The experimental ratio was 0.105.

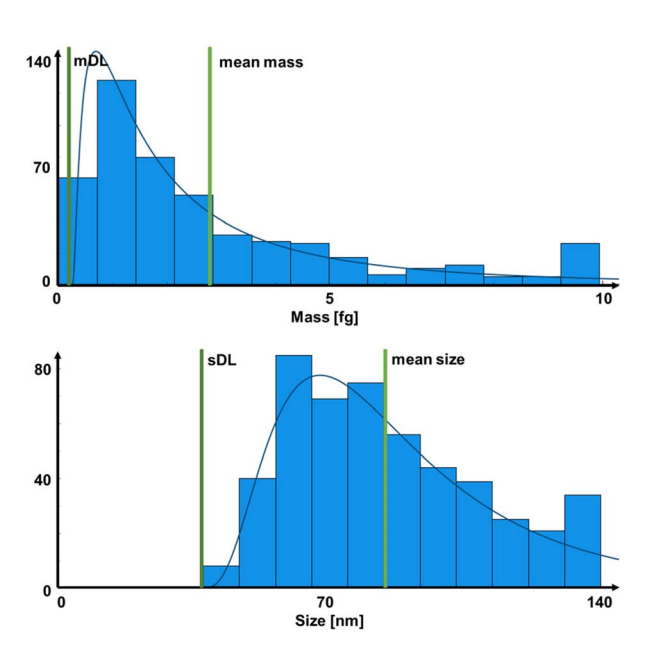


Fig. 4 The concurrent analysis of standards enabled mass and size calibrations. Shown is the mass distribution of SnO_2 NPs detected in sample W2 (left). The spherical size distribution was calculated subsequently (right). This procedure was repeated for all detected NP entities in all samples.

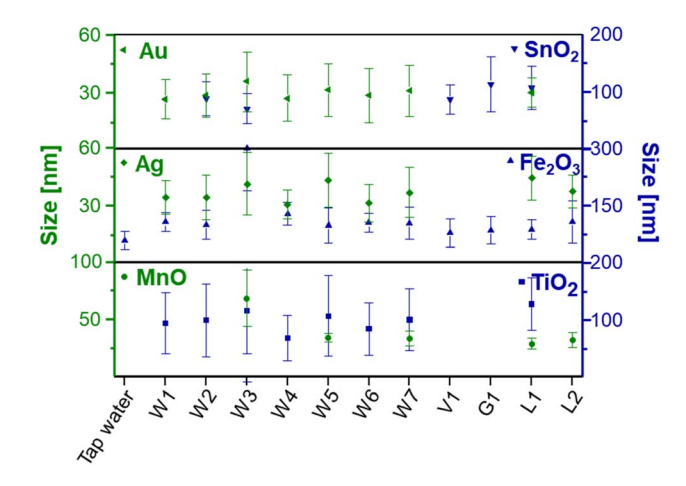


Fig. 5 Overview of selected NP identified in analysed samples. Shown are the mean size of NP entities and the standard deviations.

Conclusions

Large SP ICP-TOF-MS data sets are currently a pitfall for nontarget screening approaches to identify relevant NP entities. This work suggests the application of a novel screening tool using a LN approximation to count data points above a critical level and to indicate samples and elements with significant numbers of SP signals. The screening algorithm is detached from more dedicated algorithms, calibration, and visualisation tools to cope with large data sets and to efficiently scan through all isotopes in the detected mass range. Using either Gaussian or an LN approximation for compound Poisson statistics, elements above a minimum screening threshold are reported and may be selected for in-depth characterisation.

In a proof of concept, NPs were qualitatively and quantitatively interrogated in spirit samples. Samples were subjected to the developed screening approach and found particulate elements were calibrated to determine PNCs, figures of merit, mass and size distributions. The simultaneous acquisition capabilities of SP ICP-TOF-MS enabled the determination of isotope ratios to confirm the absence of spectral interferences and to ensure accurate calibrations. The elements Sn, Fe, Ti, Ag, Au, Cu, Zn and Mn were found in particles in spirits and tap water and the analysis of PNCs, sizes/masses and ionic background may have utility for profiling efforts.

Conflicts of interest

L. S. works for Nu Instruments.

Acknowledgements

The authors acknowledge the financial support by the University of Graz.

References

- 1 S. Bakshi, Z. L. He and W. G. Harris, Natural Nanoparticles: Implications for Environment and Human Health, *Crit. Rev. Environ. Sci. Technol.*, 2015, 45(8), 861–904, DOI: 10.1080/10643389.2014.921975.
- 2 M. F. Hochella, D. W. Mogk, J. Ranville, I. C. Allen, G. W. Luther, L. C. Marr, *et al.*, Natural, incidental, and engineered nanomaterials and their impacts on the Earth system, *Science*, 2019, 363(6434), eaau8299, DOI: 10.1126/science.aau8299.
- 3 P. P. Edwards and J. M. Thomas, Gold in a Metallic Divided State—From Faraday to Present-Day Nanoscience, *Angew. Chem., Int. Ed.*, 2007, **46**(29), 5480–5486.
- 4 S. Mourdikoudis, R. M. Pallares and N. T. K. Thanh, Characterization techniques for nanoparticles: comparison and complementarity upon studying nanoparticle properties, *Nanoscale*, 2018, **10**(27), 12871–12934.
- 5 K. P. M. McComiskey and L. Tajber, Comparison of particle size methodology and assessment of nanoparticle tracking analysis (NTA) as a tool for live monitoring of crystallisation pathways, *Eur. J. Pharm. Biopharm.*, 2018, 130, 314–326.
- 6 D. Clases and R. Gonzalez de Vega, Facets of ICP-MS and their potential in the medical sciences—Part 2: nanomedicine, immunochemistry, mass cytometry, and bioassays, *Anal. Bioanal. Chem.*, 2022, 414, 7363–7386.
- 7 D. Mozhayeva and C. Engelhard, A critical review of single particle inductively coupled plasma mass spectrometry –

- a step towards an ideal method for nanomaterial characterization, J. Anal. At. Spectrom., 2020, 35, 1740–1783.
- 8 R. Gonzalez de Vega, T. E. Lockwood, X. Xu, C. Gonzalez de Vega, J. Scholz, M. Horstmann, *et al.*, Analysis of Ti- and Pb-based particles in the aqueous environment of Melbourne (Australia) via single particle ICP-MS, *Anal. Bioanal. Chem.*, 2022, **414**, 5671–5681.
- 9 S. Meyer, R. Gonzalez de Vega, X. Xu, Z. Du, P. A. Doble and D. Clases, Characterization of Upconversion Nanoparticles by Single-Particle ICP-MS Employing a Quadrupole Mass Filter with Increased Bandpass, *Anal. Chem.*, 2020, 92(22), 15007–15016.
- 10 P. A. Doble, R. Gonzalez de Vega, D. P. Bishop, D. J. Hare and D. Clases, Laser Ablation-Inductively Coupled Plasma-Mass Spectrometry Imaging in Biology, *Chem. Rev.*, 2021, 121, 11769–11822.
- 11 M. Stupak, I. Goodall, M. Tomaniova, J. Pulkrabova and J. Hajslova, A novel approach to assess the quality and authenticity of Scotch whisky based on gas chromatography coupled to high resolution mass spectrometry, *Anal. Chim. Acta*, 2018, **1042**, 60–70.
- 12 H. H. Jeleń, M. Majcher and A. Szwengiel, Key odorants in peated malt whisky and its differentiation from other whisky types using profiling of flavor and volatile compounds, *LWT-Food Sci. Technol.*, 2019, **107**, 56–63.
- 13 P. Wiśniewska, M. Śliwińska, T. Dymerski, W. Wardencki and J. Namieśnik, Application of Gas Chromatography to Analysis of Spirit-Based Alcoholic Beverages, *Crit. Rev. Anal. Chem.*, 2015, 45(3), 201–225.
- 14 R. Winterova, R. Mikulikova, J. Mazac and P. Havelec, Assessment of the authenticity of fruit spirits by gas chromatography and stable isotope ratio analyses, *Czech J. Food Sci.*, 2008, **26**(5), 368–375.
- 15 D. W. Lachenmeier, 21 Advances in the Detection of the Adulteration of Alcoholic Beverages Including Unrecorded Alcohol, in *A in FAT*, ed. G. Downey, Woodhead Publishing Series in Food Science, Technology and Nutrition, Woodhead Publishing, 2016, pp. 565–84.
- 16 M. Gajek, A. Pawlaczyk, E. Maćkiewicz, J. Albińska, P. Wysocki, K. Jóźwik, et al., Assessment of the Authenticity of Whisky Samples Based on the Multi-Elemental and Multivariate Analysis, Foods, 2022, 11(18), 2810.
- 17 M. Gajek, A. Pawlaczyk, K. Jóźwik and M. I. Szynkowska-Jóźwik, The Elemental Fingerprints of Different Types of Whisky as Determined by ICP-OES and ICP-MS Techniques in Relation to Their Type, Age, and Origin, *Foods*, 2022, 11(11), 1616.
- 18 D. A. Magdas, G. Cristea, A. Pîrnau, I. Feher, A. R. Hategan and A. Dehelean, Authentication of Transylvanian Spirits Based on Isotope and Elemental Signatures in Conjunction with Statistical Methods, *Foods*, 2021, **10**(12), 3000.
- 19 T. E. Lockwood, R. de Vega and D. Clases, An interactive Python-based data processing platform for single particle and single cell ICP-MS, *J. Anal. At. Spectrom.*, 2021, 36(11), 2536–2544.

Paper

20 L. A. Currie, Detection: international update, and some

emerging dilemmas involving calibration, the blank, and multiple detection decisions, *Chemom. Intell. Lab. Syst.*, 1997, 37(1), 151–181.

- 21 A. Gundlach-Graham, L. Hendriks, K. Mehrabi and D. Günther, Monte Carlo Simulation of Low-Count Signals in Time-of-Flight Mass Spectrometry and Its Application to Single-Particle Detection, *Anal. Chem.*, 2018, **90**(20), 11847–11855, DOI: **10.1021/acs.analchem.8b01551**.
- 22 L. Hendriks, A. Gundlach-Graham and D. Günther, Performance of sp-ICP-TOFMS with signal distributions fitted to a compound Poisson model, *J. Anal. At. Spectrom.*, 2019, 34(9), 1900–1909.
- 23 L. Hendriks, A. Gundlach-Graham, B. Hattendorf and D. Gunther, Characterization of a new ICP-TOFMS

- instrument with continuous and discrete introduction of solutions, *I. Anal. At. Spectrom.*, 2017, 32(3), 548-561.
- 24 A. Gundlach-Graham and R. Lancaster, Mass-Dependent Critical Value Expressions for Particle Finding in Single-Particle ICP-TOFMS, *Anal. Chem.*, 2023, **95**(13), 5618–5626.
- 25 L. Fenton, The Sum of Log-Normal Probability Distributions in Scatter Transmission Systems, *IRE Trans. Commun. Syst.*, 1960, **8**(1), 57–67.
- 26 P. Westerhoff, A. Atkinson, J. Fortner, M. S. Wong, J. Zimmerman, J. Gardea-Torresdey, *et al.*, Low risk posed by engineered and incidental nanoparticles in drinking water, *Nat. Nanotechnol.*, 2018, 13(8), 661–669.
- 27 C. Couto and A. Almeida, Metallic Nanoparticles in the Food Sector: A Mini-Review, *Foods*, 2022, **11**(3), 402.